Performance enhancement of the 2-D wavelength-hopping/time-spreading synchronous OCDM system using a heterodyne detection receiver and PPM signaling

Anh T. Pham[1,*] and Hiroyuki Yashima[2]

[1]*The University of Aizu, Aizu-Wakamatsu City, Fukushima 965-8580, Japan*
[2]*Tokyo University of Science, 1-3 Kagurazaka, Shinjuku-ku, Tokyo 162-8601, Japan*
[*]*Corresponding author: pham@u-aizu.ac.jp*

Received November 1, 2006; revised February 5, 2007;
accepted April 16, 2007; published May 31, 2007 (Doc. ID 76594)

Two-dimensional wavelength-hopping/time-spreading synchronous optical code-division multiplexing systems using a heterodyne detection receiver and pulse-position modulation (PPM) signaling are investigated. Prime sequences are used as signature code for both wavelength hopping and time spreading. Performance of the proposed systems is theoretically analyzed taking into account various kinds of noise and interference, including multiple access interference, optical beating interference, crosstalk, and receiver noise. We also compare the performance of the proposed systems with the conventional ones using ON–OFF keying signaling. Numerical results show the improvement in both number of users and optical power gain with a proper selection of PPM word length M. © 2007 Optical Society of America

OCIS codes: 060.0060, 060.4230, 060.2360.

1. Introduction

Over the past decade or so, optical code-division multiplexing (OCDM) has been considered an attractive candidate for the next generation last mile broadband optical networks. This is thanks to its many advantages, such as fully asynchronous access, soft capacity limit, differentiated service at physical layer, decentralized network control, and increased security [1,2]. In OCDM systems, the transmitted signal can be optically encoded (i.e., spread) in either time or frequency domain. Such systems are called one-dimensional (1-D) systems. One of the major issues in the 1-D OCDM systems is the limitation of code cardinality due to the high-cross-correlation in unipolar spreading codes. To solve this problem, a new class of two-dimensional (2-D) codes has been recently proposed for OCDM systems, in which the transmitted signal is encoded by using a combination of wavelength hopping (WH) and time spreading (TS) [3].

In OCDM systems that use frequency domain to encode the transmitted signal, it is seen that optical beating interference (OBI), which occurs when a photodetector simultaneously receives two or more optical waves with nearly the same wavelength, is the dominant noise that seriously affects the system performance [4,5]. In 2-D WH/TS OCDM systems, the effect of OBI is also critical; it is shown in [6] that OBI can sizably reduce the number of simultaneous users to less than a third.

A heterodyne detection receiver was recently proposed for use in 2-D WH/TS OCDM systems as an effort to reduce the effect of OBI and to improve the system performance [7]. In this paper, pulse-position modulation (PPM) signaling is additionally proposed in order to further enhance the performance of the 2-D WH/TS OCDM systems. PPM is an optical block encoding technique in which an optical pulse is placed in one of M adjacent time slots to represent the data block. PPM signaling was proposed for 1-D OCDM systems, and it was proved to be able to improve the system performance [8,9]. In our analysis, we consider most major noise and interferences in the proposed systems, including multiple access interference (MAI), OBI, crosstalk, and receiver noise under the assumption of ideal heterodyne detection without phase fluctuation and prior synchronization of PPM symbols. We will show that the PPM signaling, with a proper selection of word length M, can further improve the performance of

1536-5379/07/060789-12/$15.00

the 2-D WH/TS OCDM systems, increase the number of users, and offer a significant optical power gain.

The rest of the paper is organized as follows. Section 2 presents the descriptions of the conventional 2-D WH/TS OCDM systems using ON–OFF keying (OOK) and our proposed systems using a heterodyne detection receiver and PPM signaling. The performance analysis and numerical results are presented in Sections 3 and 4, respectively. Finally, Section 5 concludes the paper.

2. System Descriptions

2.A. Direct Detection 2-D WH/TS OCDM System Using OOK Signaling

Figure 1 shows a pair of a transmitter and receiver in the direct detection 2-D WH/TS OCDM system using OOK signaling. The optical broadband source (multicarrier) at the transmitter is assumed to be ideally flat spectra over the optical bandwidth. In this system, binary data is used to modulate the broadband source to generate ON–OFF pulses. These pulses are then 2-D encoded by spreading in time domain and hopping their wavelength components in the frequency domain. There are several classes of 2-D WH/TS code such as extended quadratic congruence (eqc) sequences [3], codes generated from "depth-first search algorithm" [10], pseudoorthogonal matrix codes [11], and extended carrier-hopping prime codes [12]. In this paper, we use the prime sequences code that is the most popular and widely studied [13]. For a given set of prime numbers p_h, p_s, with $p_s \leq p_h$, we can create a set of WH/TS hopping sequences whose cardinality of $p_s \times (p_h - 1)$, maximum cross correlation of one and zero sidelobes autocorrelation. An example of WH/TS code when $p_s = p_h = 5$ is shown in Fig. 2. In this figure, a single spreading pattern of (10000 01000 00100 00010 00001) is used for four (i.e., $p_h - 1$) hopping patterns. Further information about the code construction can be found in [3,13].

The WH/TS encoder can be constructed of fiber Bragg gratings (FBGs) as shown in Fig. 3(a). At the transmitter, wavelength components of data-carried OOK signal are first spread into chip pulses at the encoder. These chip pulses are time delayed in line with the positions of the FBGs, which correspond to the time-spreading pattern of a signature code generated locally at the code generator. These FBGs are also tuned to different wavelengths corresponding to the hopping pattern of the signature code. At the encoder's output, wavelength components are then combined to create a WH/TS encoded signal. The signal is finally transmitted into an optical multiple access channel together with signals from other users.

At the receiver, the WH/TS decoder is also constructed of FBGs, as shown in Fig. 3(b). These FBGs are, however, tuned in inverse order of those in the encoder of the targeted transmitter. The decoder can be configured to receive data from other users by tuning the wavelengths in the FBGs to the desired user's corresponding signature code. By passing through the decoder, wavelength components from the targeted user will be matched and reconstructed by canceling the relative time delay among pulses. Components from interfering users cause MAI, which is determined by the cross-correlation feature of the code family (which is at most one in the considered

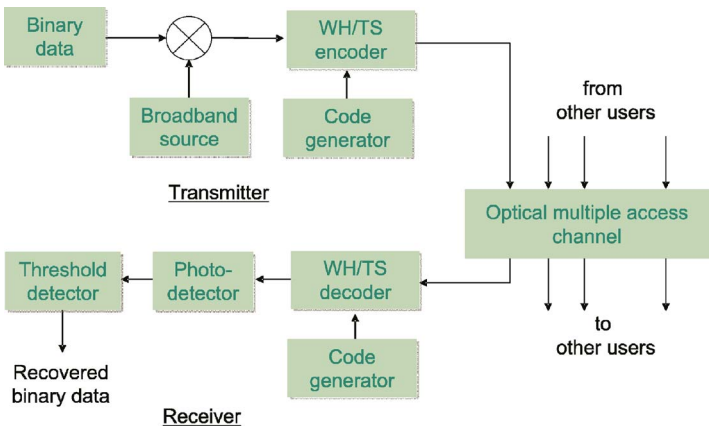

Fig. 1. Pair of transmitter and receiver in the direct detection 2-D WH/TS OCDM system using OOK signaling.

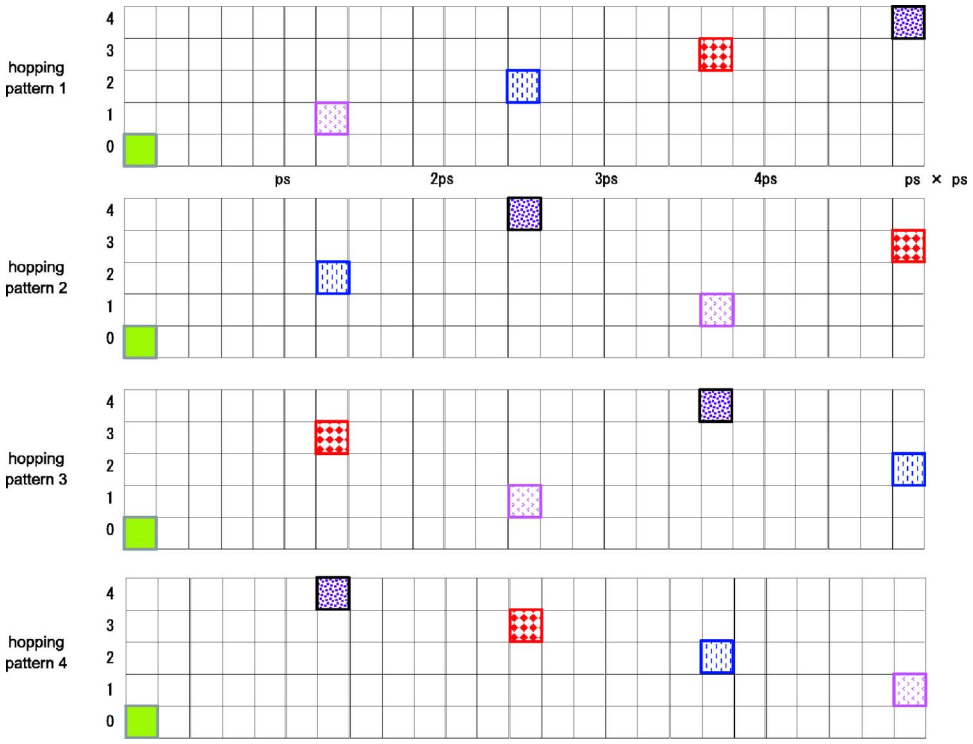

Fig. 2. (p_h-1) wavelength-hopping patterns created from a single time-spreading pattern when $p_s=p_h=5$.

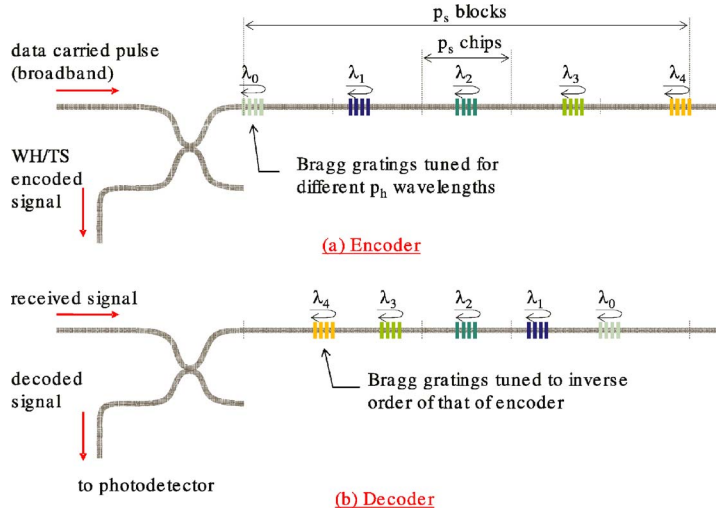

Fig. 3. FBG-based encoder and decoder.

system). The decoded signal is converted into an electrical signal by a photodetector. It is at the photodetector where OBI arises when waves with close wavelengths beat each other. Binary data is finally recovered by a threshold detector where binary bit "1" or "0" is decided depending upon whether the integrated current over a bit period is higher or lower than a preset threshold level.

2.B. 2-D WH/TS OCDM System Using a Heterodyne Detection Receiver and PPM Signaling

Figure 4 describes a pair of a transmitter and receiver in the proposed 2-D WH/TS OCDM system using a heterodyne detection receiver and PPM signaling. Blocks of $\log_2(M)$ binary data are first encoded into M-ary symbols, denoted as s $(s \in \{0,\ldots,M-1\})$. The broadband optical signal is then position modulated to one of M disjoint time slots corresponding with the M-ary symbols. The M-ary symbol is then encoded

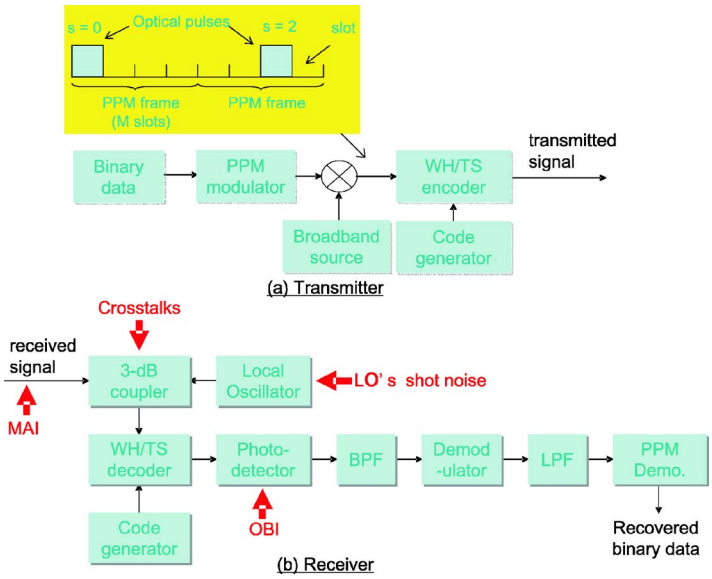

Fig. 4. Proposed 2-D WH/TS OCDM system using a heterodyne detection receiver and PPM signaling.

and transmitted in a similar way to that of the conventional direct detection 2-D WH/TS OCDM system using OOK signaling.

At the receiver, the received signal (including MAI) is first mixed coherently with a local oscillator (LO). This LO is also a broadband source whose characteristics (spectra, wavelength components, and separation between them) are the same as the one at the transmitter. The mixed signal is decoded at the WH/TS decoder in a similar way as in the OOK system then detected by a photodetector. The photocurrent is passed through a bandpass filter (BPF), converted to baseband by multiplying with the recovered carrier (synchronous demodulation), then followed by a low-pass filter (LPF). Finally, at the PPM demodulator, integrated photocurrent over M slots are compared, and the position of the slot with the highest current determines the transmitted symbol.

As depicted in Fig. 4, there are several kinds of noises and interferences that appear in the received photocurrent, including MAI, OBI, crosstalk arising from signal mixing at the receiver, and the receiver noise. In Section 3, we will present the system performance analysis considering all those noise and interferences.

3. System Performance Analysis

In this section, we will theoretically analyze the performance of the proposed system and derive its bit error rate (BER). To do so, the received signal spectra is first analyzed to understand the statistical nature of the photocurrent at the output of the photodetector. BER is then derived taking into account MAI, OBI, crosstalk, and receiver noise.

3.A. Signal Spectra Analysis

In the following analysis, we assume the chip synchronous (upper bound performance) for all users. Also, for the sake of simplicity, PPM slots are also assumed to be prior synchronized.

We first consider the photocurrent caused by a single wavelength component. Denote $\omega_{c\text{-}d}$ and $\phi_{c\text{-}d}$ as frequency and phase of a specific wavelength component from the desired user ($c=1,\ldots,p_h$). Assume that there are K simultaneous users in the network; and at a given instant time, there are μ_c users that cause interference at $\omega_{c\text{-}d}$. As well, denote frequency and phase of the wavelength component from ith interfering user ($i=1,2,\ldots,\mu_c$) as $\omega_{c\text{-}i}$ and $\phi_{c\text{-}i}$, the optical field associated with the desired wavelength component and its interfering pulses, E_s, can be written as

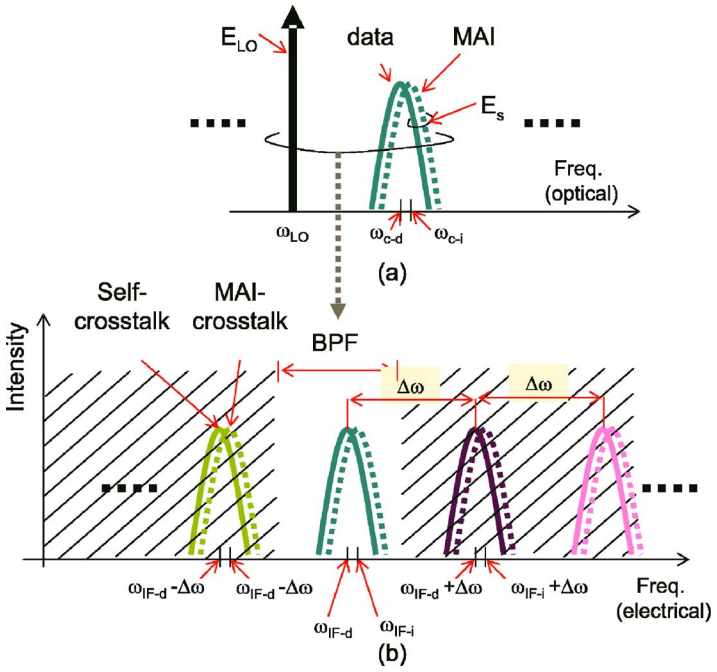

Fig. 5. (a) Optical spectra of E_{LO} and E_s (interfering user ith only), and (b) the electrical spectra at photodetector output.

$$E_s = \sqrt{P_d}\exp[j(\omega_{c\text{-}d}t + \phi_{i\text{-}d})] + \sum_{i=1}^{\mu_c}\sqrt{P_i}\exp[j(\omega_{c\text{-}i}t + \phi_{c\text{-}i})], \tag{1}$$

where P_d and P_i are optical power of wavelength components from desired and interfering user ith, respectively.

The LO wavelength component corresponding to $\omega_{c\text{-}d}$, ω_{LO}, is chosen so that the intermediate frequency (IF) $\omega_{\mathrm{IF}\text{-}d} = \omega_{c\text{-}d} - \omega_{\mathrm{LO}}$ is in the microwave region, i.e., ~1 GHz. The optical field associated with ω_{LO}, denoted as E_{LO}, can also be written as

$$E_{\mathrm{LO}} = \sqrt{P_{\mathrm{LO}}}\exp[j(\omega_{\mathrm{LO}}t + \phi_{\mathrm{LO}})], \tag{2}$$

where P_{LO} and ϕ_{LO} are power and phase of the LO's wavelength component.

We assume that there is the same separation between two adjacent wavelength components in LO or any user, and denote it as $\Delta\omega$. Figure 5(a) describes the optical spectra of LO, data and MAI (only the considered component); Fig. 5(b) shows the electrical spectra at the photodetector output, which includes IF components of data and MAI, and crosstalk. Note that crosstalk is caused by the beating between ω_{LO} with other components in the useful data and MAI signal. Thus, there are self-, and MAI crosstalk components that are $\pm n\Delta\omega$ ($n = 1, 2, \ldots$) differed from IF. By using an electronic BPF the crosstalk components can be removed, provided that $\Delta\omega$ exceeds the two times electrical bandwidth. Therefore, the heterodyne photocurrent (responsivity $\Re$) at a given time, after removing the nearly constant direct-current (DC) component (since $P_{\mathrm{LO}} \gg P_d, P_i$) and crosstalk, can be expressed as

$$\begin{aligned} i(t) = {} & \underbrace{2\Re\sqrt{P_{\mathrm{LO}}P_d}\cos(\omega_{\mathrm{IF}\text{-}d}t + \phi_{c\text{-}d} - \phi_{\mathrm{LO}})}_{\text{data}} \\ & + \underbrace{2\Re\sum_{i=1}^{\mu_c}\sqrt{P_{\mathrm{LO}}P_i}\cos(\omega_{\mathrm{IF}\text{-}i}t + \phi_{c\text{-}i} - \phi_{\mathrm{LO}})}_{\text{MAI}} + \underbrace{2\Re\sum_{i=1}^{\mu_c}\sqrt{P_dP_i}\cos[(\omega_{c\text{-}d} - \omega_{c\text{-}i})t + \phi_{c\text{-}d} - \phi_{c\text{-}i}]}_{\text{primary OBI}} \\ & + \underbrace{2\Re\sum_{j=i+1}^{\mu_c}\sum_{i=1}^{\mu_c-1}\sqrt{P_iP_j}\cos[(\omega_{c\text{-}i} - \omega_{c\text{-}j})t + \phi_{c\text{-}i} - \phi_{c\text{-}j}]}_{\text{secondary OBI}}. \end{aligned} \tag{3}$$

Here, $\omega_{\text{IF-}i}=\omega_{c\text{-}i}-\omega_{\text{LO}}$ is the IF from interference ith.

For the sake of simplicity, the ideal heterodyne detection without phase fluctuation is assumed. In the case when the heterodyne detection is synchronous (i.e., by using carrier recovery at IF), the total photocurrent in slot uth ($u \in \{0,\ldots,M-1\}$), denoted as I_u, can be given by

$$I_u = I_c^{(u)} + i_{\text{OBI}}^{(u)}, \tag{4}$$

where the first term is signal contributed from useful data and MAI, which, from Eq. (3), can be given by

$$I_c^{(u)} = \Re\sqrt{2P_{\text{LO}}P_s}(bp_s + \iota_u), \tag{5}$$

where $b=1$ when $s=u$ with s is the transmitted M-ary symbol, otherwise $b=0$. $\iota_u=\Sigma_{p_s}\mu_c$ is the number of interfering pulses in slot uth (each user uses p_s in total of p_h wavelengths); here we assume that all users have the same optical power level $P_d=P_i=P_s$. The second term of Eq. (4), which is contributed from OBI (both primary and secondary), causes the fluctuation in the received photocurrent in slot uth. As the probability density function (pdf) of OBI approaches Gaussian in the presence of multiple interferences [14], $i_{\text{OBI}}^{(u)}$ can be modeled as zero-mean Gaussian random variable with variances denoted as δ_{OBI}^2. From Eq. (3), the OBI noise power in uth slot can be derived as

$$\delta_{\text{OBI}}^2 = B_e\tau_c(I_{\text{OBI}_{pr}}^2 + I_{\text{OBI}_{se}}^2) = 2B_e\tau_c\Re^2P_s^2\left[b\iota_u + \sum_{p_s}\binom{\mu_c}{2}\right], \tag{6}$$

where B_e is the receiver electrical bandwidth and τ_c is the coherent time of the broadband source, which can be approximate as $\tau_c=1/B_o$ where B_o is the optical bandwidth of the source and ι_u is the number of interfering pulses in slot uth. Here, it is noted that the primary OBI presents only when there is useful data transmitted in slot u (e.g., $b=1$).

To calculate OBI noise power, distribution of ι_u over p_s wavelength components in slot uth should be considered. Denote $\mu=(\mu_0,\mu_1,\ldots,\mu_{p_s})$ as the p_s dimensional vector that represents the distribution of ι_u interfering pulses over p_s wavelength components. It is seen that μ is a random variable that can be modeled as a multinomial distribution with an equal probability $P_i=1/p_s$ [6]. By averaging the secondary OBI component in Eq. (6) over μ, the OBI noise power can be given as

$$\delta_{\text{OBI}}^2 = 2B_e\tau_c\Re^2P_s^2\left[b\iota_u + \frac{1}{p_s}\binom{\iota_u}{2}\right]. \tag{7}$$

As a result, total noise power (including OBI and receiver noise) in slot uth, denoted as δ_u^2, can be given as

$$\delta_u^2 = \delta_{\text{OBI}}^2 + \delta_{rx}^2, \tag{8}$$

where δ_{rx}^2, the receiver noise power, includes the contribution from both shot noise and thermal noise, and can be given as

$$\delta_{rx}^2 = \delta_{th}^2 + \delta_{sh}^2, \tag{9}$$

where thermal noise $\delta_{th}^2=8\pi k_BT_nB_e^2C$ and shot noise $\delta_{sh}^2=2p_seB_e\Re P_{LO}$ (note that the shot noise from the p_s LOs is dominant as $P_{LO}\gg P_s$). Here k_B is Boltzman's constant, T_n is the receiver noise temperature, C is the receiver capacitor, and e is the electron charge.

3.B. System BER

In the proposed system, errors happen when the PPM demodulator wrongly declares the transmitted symbol. Given a symbol error rate P_e, the BER can be interpreted as [15]:

$$\text{BER} = \frac{M/2}{M-1}P_e. \tag{10}$$

We assume that the transmitted data is large enough so that the transmitted symbols are equally distributed over M slots, i.e., probability that $s=u$ $(u \in \{0,\ldots,M-1\})$, $\Pr(s=u)=1/M$. Without loss of generality, we also assume the transmitted symbol $s=0$. Employing a union bound, the symbol error rate P_e can be given as

$$P_e \le 1-\Pr\{I_0 > I_u | u \in \{1,\ldots,M-1\}, s=0\} \le \sum_{u=1}^{M-1} \Pr\{I_u \ge I_0 | s=0\} = (M-1)\Pr\{I_1 \ge I_0 | s = 0\} = (M-1)\sum_{l_0=0}^{K-1}\sum_{l_1=0}^{K-l_0-1} \Pr\{\kappa_0=l_0,\kappa_1=l_1\} \times \Pr\{I_1 \ge I_0 | s=0,l_0,l_1\}, \tag{11}$$

where I_u is total photocurrent in slot uth, as given in Eq. (3), s represents the transmitted symbol. κ_u is the random variable that represents the number of users whose transmitted symbol $s=u$, which is a binomial variable [8]. The first term in Eq. (11), the probability that $\kappa_0=l_0$ and $\kappa_1=l_1$, can be expressed as

$$\Pr\{\kappa_0=l_0,\kappa_1=l_1\} = \sum_{l_2,\ldots,l_{M-1}} \Pr\{\kappa_0=l_0,\ldots,\kappa_{M-1}=l_{M-1}\}, = \binom{K-1}{l_0}\left(\frac{1}{M}\right)^{l_0}\left(1-\frac{1}{M}\right)^{K-1-l_0}\binom{K-1-l_0}{l_0}\left(\frac{1}{M-1}\right)^{l_1}\left(1-\frac{1}{M-1}\right)^{K-1-l_0-l_1}. \tag{12}$$

In a given slot, a pulse from interfering users will become an interfering one when it matches both position and wavelength with the FBG in the WH/TS decoder. Denote ζ_u as the random variable that represents the total number of interfering pulses to p_s wavelength in slot u. ζ_u can be modeled as a binomial random variable with probability (μ_λ/p_s^2) where μ_λ is the average number of wavelengths common to a pair of signature codes, which, in case of prime sequences, can be estimated as [3]:

$$\mu_\lambda = \frac{1}{\binom{p_h}{p_s}}\left\{\binom{p_h-1}{p_s-1}\frac{(p_s-1)(p_s-2)+(p_h-2)}{p_h-2} + \binom{p_h-1}{p_s}\frac{p_s(p_s-1)}{p_h-2}\right\}. \tag{13}$$

Therefore, the pdf of the random variable ζ_u, given the total number of interfering user l_u, can be given as

$$\Pr(\zeta_u = \iota_u | l_u) = \binom{l_u}{\iota_u}\left(\frac{\mu_\lambda}{p_s^2}\right)^{\iota_u}\left(1-\frac{\mu_\lambda}{p_s^2}\right)^{l_u-\iota_u}. \tag{14}$$

From the above equation and Eqs. (4)–(9), the second portion in Eq. (11) therefore can be derived as

$$\Pr\{I_1 \ge I_0 | s=0,l_0,l_1\} = \sum_{i=0}^{l_0}\Pr\{\zeta_0 = i|l_0\}\sum_{j=0}^{l_1}\Pr\{\zeta_1=j|l_1\}Q\left(\frac{I_c^{(0)}-I_c^{(1)}}{\sqrt{\delta_1^2+\delta_0^2}}\right) = \sum_{i=0}^{l_0}\Pr\{\zeta_0 = i|l_0\}\sum_{j=0}^{l_1}\Pr\{\zeta_1=j|l_1\} \times Q\left\{\frac{\Re\sqrt{2P_{LO}P_s}(p_s+i-j)}{\sqrt{2B_e\tau_c R^2 P_s^2\left[i+\frac{1}{p_s}\binom{i}{2}+\frac{1}{p_s}\binom{j}{2}\right]+2\delta_{rx}^2}}\right\}, \tag{15}$$

with

$$Q(x) = \frac{1}{\sqrt{2\pi}}\int_x^{+\infty} e^{-y^2/2}\mathrm{d}y.$$

Finally, from Eqs. (11), (12), and (15), we can calculate the symbol error rate P_e and then convert into the BER using Eq. (10).

4. Numerical Results

In this section, we present the numerical results that highlight the advantages of the proposed system over the conventional one using OOK signaling with and without a

Table 1. System Parameters and Constants

Name	Symbol	Value
Boltzmann's constant	k_B	1.38054×10^{-23} W/K/Hz
Electron charge	e	1.6×10^{-19} C
Light velocity	c	3×10^{8} m/s
Receiver capacitor	C	0.02×10^{-12} F
Receiver noise temperature	T_n	300 K
Photodetector responsivity	$\Re$	1 A/W
Optical bandwidth	B_o	2.5 THz
WH and TS prime numbers	p_s,p_h	13
LO optical power	P_{LO}	0 dBm

heterodyne detection receiver. The performance data of the OOK system is taken from [7]. The system parameters and constants used in this section are shown in Table 1.

As the PPM signaling can be considered as a coding with rate of $\log_2(M)/M$, when the binary data rate R_b= constant, the PPM slot width $T_s=T_b[\log_2(M)/M]$, where $T_b=1/R_b$ is the duration of a bit in the OOK system. The receiver electrical bandwidth B_e required in the PPM system is thus $M/\log_2(M)$ times wider as compared with the OOK counterpart. Also, in order to have a fair comparison between the proposed systems and conventional one using OOK, the numerical results are considered under a constraint on average signal power, i.e., fixed power per information bit. Under this constraint, the optical power per pulse (wavelength component) in PPM system can be derived in relation with the received optical power per bit, denoted as P_o, as

$$P_s = P_o \frac{\log_2(M)}{Mp_s}. \tag{16}$$

First, Fig. 6 shows the system's BER versus the number of users when the optical power per bit (a) $P_o=-45$ dBm and (b) $P_o=-42$ dBm. The proposed systems with different M are compared with the conventional system using OOK with and without a heterodyne detection receiver. The user bit rate is $R_b=10$ Gbits/s. It is seen that the proposed system offers better performance than that of conventional ones. System

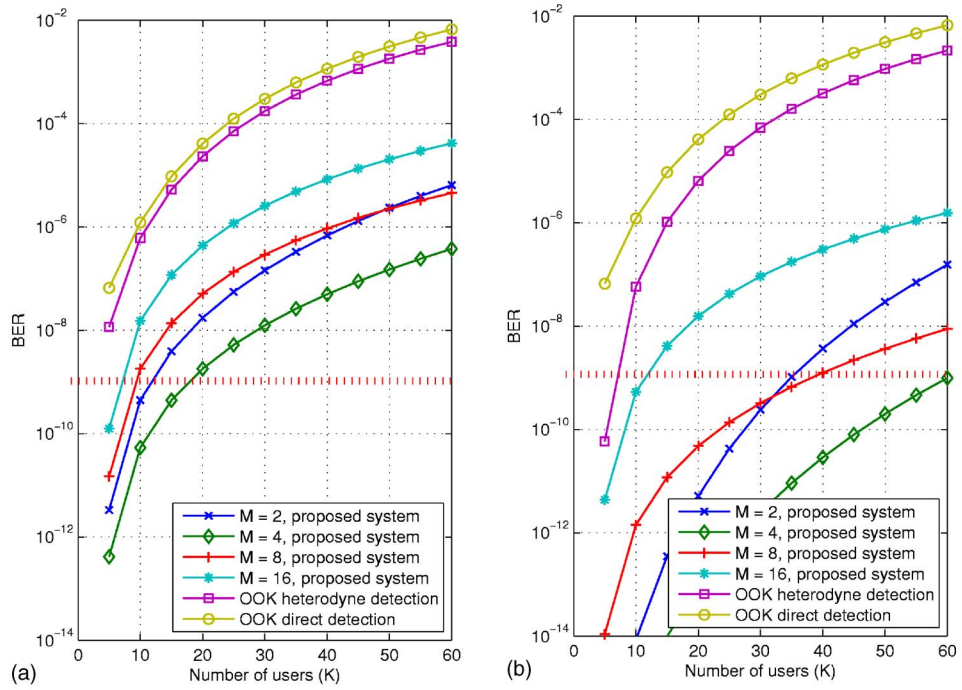

Fig. 6. BER versus K when (a) $P_o=-45$ dBm, and (b) $P_o=-42$ dBm, proposed system with $M=2$, 4, 8, and 16, compared with the conventional systems using OOK with and without a heterodyne detection receiver.

performance is improved when M is increased from 2 to 4, especially in case $P_o = -42$ dBm. As shown in Fig. 6(b), the number of users is significantly increased, from less than 10 users in the OOK system with a heterodyne detection receiver to 35 users and more than 60 users when $M = 2$ and 4, respectively.

When $M > 4$, it is seen that system performance is not improved but worsens, especially when the number of users is not large. This is due to the effect of PPM on OBI and MAI. When the number of users is small, MAI and OBI are negligible as they are dominated by shot noise. Thus, under a constraint on the optical power per bit, the optical power per pulse is decreased when M increases. Therefore, the performance of the system with higher P_s (i.e., lower M) becomes superior. On the other hand, when the number of users increases, the effect of MAI and OBI gradually becomes greater (in comparison with shot noise), especially in case P_o is higher. As PPM can relieve MAI and OBI (interfering pulses are more distributed when M increases), we can see an improvement in the system using a higher M. For example, when $K = 50$, the system with $M = 8$ outperforms the one with $M = 2$ in case $P_o = -45$ dBm. In case $P_o = -42$ dBm, this circumstance happens only at $K = 30$ as the effect of MAI and OBI is stronger when the optical power is higher.

Nevertheless, the effect of OBI and MAI become negligible (compared with LO shot noise) when we continue to increase M (as optical power per chip pulse decreases). Therefore, when $M = 16$, the system performance is the worst in both cases.

Next, Fig. 7 shows the system's BER against P_o when $K = 32$ and $R_b = 10$ Gbits/s. We can see more than 15 dB gain in the system with $M = 4$ compared with the OOK system. System performance is almost similar in the systems using $M = 2$ and 8. Compared with the system using $M = 4$, an additional 1.5 dB optical power per bit is additionally required. When $M = 16$, it is seen that about 4.5 dB higher optical power is necessary. Together with the fact that the system is more complex with higher M, it is recommended not to use $M > 4$ in the proposed system.

Figure 8 shows the relation between the required optical power per bit and K when the system's BER $= 10^{-9}$ and $R_b = 10$ Gbits/s. Again we see the smallest power required in the system using $M = 4$. Obviously, when the number of users increases, the higher optical power is required. It is seen that while the increased power level is high in the system with $M = 2$, it is moderate in the system using $M = 4$ and even less in the one using $M = 8$. This confirms the fact that PPM can help to relieve the effects of MAI and OBI.

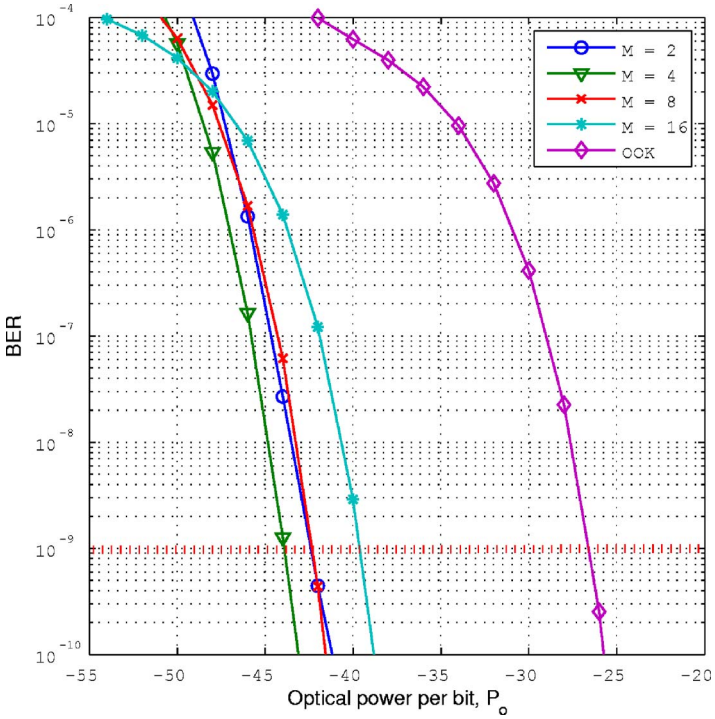

Fig. 7. BER versus P_o when $K = 32$ users. The proposed system with $M = 2$, 4, 8, and 16 compared with the conventional system using OOK with a heterodyne detection receiver.

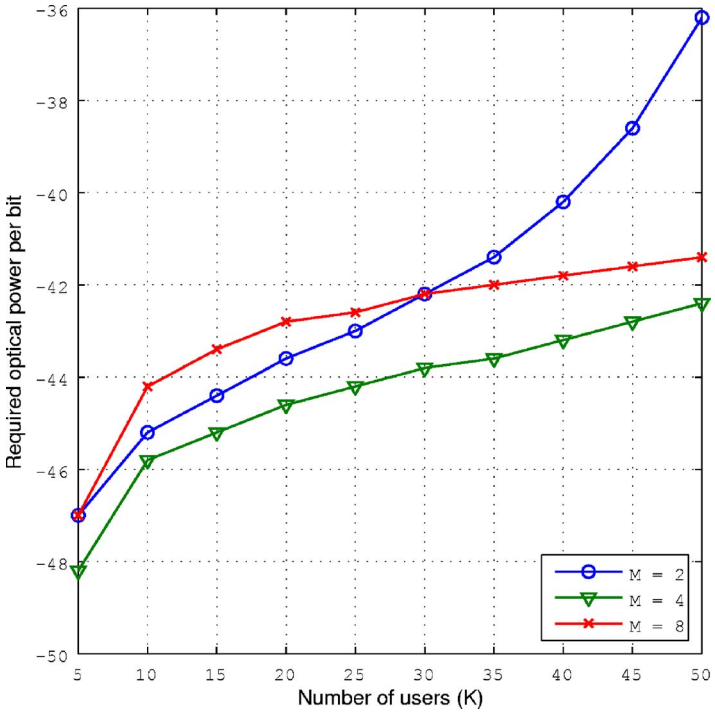

Fig. 8. Required optical power per bit P_o versus K when BER$=10^{-9}$ and R_b $=10$ Gbits/s. The proposed system using PPM signaling when $M=2$, 4, and 8.

Finally, we compare the performance limits of the proposed system with different M and the conventional system using OOK when the optical power per bit $P_o=-45$ dBm in Fig. 9(b). The calculation of network capacity, denoted as $C_N=K\times R_{b_{\max}}$, is performed when the BER$=10^{-9}$. We realize that the network capacity in the proposed system is essentially higher than that of the OOK system. The network capacity in the proposed system increases as the number of users increases. There is then an optimum number of users where the network capacity is at its maximum, e.g., at

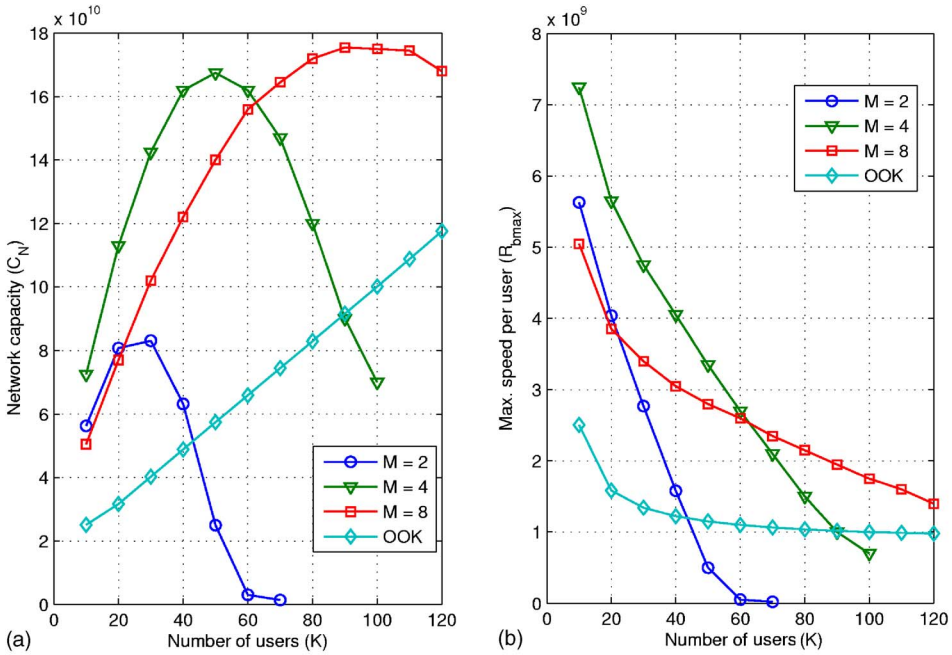

Fig. 9. (a) Network capacity versus K and (b) maximum speed per user versus K when BER$=10^{-9}$. Conventional system using OOK and the proposed system using PPM signaling when $M=2$, 4, and 8.

$K=50$ when $M=4$; the network capacity starts decreasing as the number of users continues to increase. Conversely, it is seen that the network capacity in the conventional system using OOK and a heterodyne detection receiver is low when the number of users is not large and gradually increases as the number of users increases.

The result can be clarified using Fig. 9(b). In this figure, the maximum speed per user is calculated also for the case BER$=10^{-9}$. It is obvious that in any system, the maximum speed per user is decreased as the number of users increases. However, the decrease level is different. In the system using OOK, when the number of users increases, the maximum speed is slowly decreased, which results in a gradual increase in the network capacity. The decrease of the maximum speed is more rapid in the proposed system using PPM signaling, especially when PPM word length M is small. This is because of the fact that with the same optical power level, higher M system is more relieved from OBI and MAI, which are increased when the number of users increases.

5. Conclusion

We proposed novel, to the best of our knowledge, 2-D WH/TS synchronous OCDM systems using a heterodyne detection receiver and PPM signaling. The system performance was carried out taking into account various kinds of noise and interference, including MAI, OBI, crosstalk, and receiver noise, and under the assumption of ideal heterodyne detection and prior symbol synchronization. We compared the performance of the proposed system with the conventional system using OOK signaling with and without a heterodyne detection receiver. Results show a significant improvement in both the system capacity and the required optical power. In particular, when the PPM signaling with $M=4$ is used, the number of users can be more than six times increased when optical power per bit $P_o=-42$ dBm; and an optical power gain of 15 dB is achieved in comparison with the OOK case when there are 32×10 Gbits/s users. It is seen that it is not worth it to use $M>4$ in the proposed system. In addition, we also investigated to find out the optimum number of users where the maximum network capacity can be achieved with an acceptable performance (i.e., BER$=10^{-9}$).

Acknowledgments

The authors thank the reviewers for their thorough reviews and useful suggestions for improving the readability of this paper. This work was supported in part by the Japan Society for Promotion of Science under grants-in-aid 18760278.

References and Links

1. A. Stok and E. H. Sargent, "Lighting the local area optical code-division multiple access and quality of service provisioning," IEEE Netw. **11-12**, 42–46 (2000).
2. A. Stok and E. H. Sargent, "The role of optical CDMA in access networks," IEEE Commun. Mag. **9**, 83–87 (2002).
3. L. Tancevski and I. Andonovic, "Hybrid wavelength hopping/time spreading schemes for use in massive optical networks with increased security," J. Lightwave Technol. **14**, 2636–2647 (1996).
4. E. D. J. Smith, P. T. Gough, and D. P. Taylor, "Noise limits of optical spectral-encoding CDMA systems," Electron. Lett. **31**, 1469–1470 (1995).
5. X. Wang and K. Kitayama, "Analysis of beat noise in coherent and incoherent time-spreading OCDMA," J. Lightwave Technol. **22**, 2226–2232 (2004).
6. L. Tancevski and L. A. Rusch, "Impact of the beat noise on the performance of 2-D optical CDMA systems," IEEE Commun. Lett. **4**, 264–266 (2000).
7. A. T. Pham and H. Yashima, "Performance analysis of 2-D WH/TS OCDM systems using prime sequences and a heterodyne detection receiver," in *Proceedings of the 49th Annual IEEE Global Telecommunications Conference* (IEEE, 2006).
8. H. M. H. Shalaby, "Performance analysis of optical synchronous CDMA communication systems with PPM signaling," IEEE Trans. Commun. **43**, 624–634 (1995).
9. E. D. J. Smith, R. J. Blaikie, and D. P. Taylor, "Performance enhancement of spectral-amplitude-coding optical CDMA using pulse-position modulation," IEEE Trans. Commun. **46**, 1176–1185 (1998).
10. R. M. H. Yim, L. R. Chen, and J. Bajcsy, "Design and performance of 2-D codes for wavelength-time optical CDMA," IEEE Photon. Technol. Lett. **14**, 714–716 (2002).
11. A. J. Mendez, R. M. Gagliardi, V. J. Hernandez, C. V. Bennett, and W. J. Lennon, "Design and performance analysis of wavelength/time (W/T) matrix codes for optical CDMA," J. Lightwave Technol. **21**, 2524–2533 (2003).

12. W. C. Kwong and G.-C. Yang, "Extended carrier-hopping prime codes for wavelength-time optical code-division multiple access," IEEE Trans. Commun. **52**, 1084–1091 (2004).
13. G.-C. Yang and W. C. Kwong, *Prime Codes With Applications to CDMA Optical and Wireless Networks* (Artech House, 2002).
14. A. Aria, M. Tur, and E. L. Goldstein, "Probability-density function of noise at the output of a two beam interferometer," J. Opt. Soc. Am. A **8**, 1936–1942 (1991).
15. R. M. Gagliardi and S. Karp, *Optical Communications*, 2nd ed. (Wiley Interscience, 1995).